

# Strength and fracture behaviour of diffusion bonded joints in Al–Li (8090) alloy

## Part III Peel strength

D. V. DUNFORD, P. G. PARTRIDGE

Materials and Structures Department DRA, Aerospace Division, Royal Aerospace Establishment Farnborough, Hampshire, GU14 6TD, UK

Peel strengths at room temperature and under superplastic forming conditions at 530 °C were measured for diffusion-bonded joints in Al–Li 8090 alloy sheet. The bonds were made in the solid state, or via a transient liquid phase using interlayers. The effect of strain rate, sheet thickness and heat treatment were investigated. The significance of these results for the testing of DB joints and for their use in DB/SPF structures is discussed.

### 1. Introduction

Superplastic forming (SPF) has become an important processing option for Al–Li 8090 alloy sheet structures [1]. Since high-strength joints have been obtained by diffusion bonding (DB) [2–5], there has been considerable interest in DB/SPF processing of this alloy in order to manufacture low-cost, low-density sheet structures as demonstrated for titanium alloy sheet [6]. There is, however, significant scatter in reported shear strength data for DB joints in aluminium alloys [2]. This may be attributed to different bonding and testing techniques, and to differences in surface preparation or contamination prior to bonding. In practice, bond peel tests at room and elevated temperatures more closely reflect the processing and service loading conditions for DB/SPF structures, but unfortunately, peel strength is particularly sensitive to the test technique [7]. Parts I [2] and II [8] of this paper described the shear strength and fracture behaviour of DB joints in 8090 alloy sheet. In Part III the results of a bond peel test programme are described and compared with other published data. Both solid state and transient liquid-phase bonds were tested at room temperature and at the superplastic forming temperature of 530 °C.

### 2. Experimental procedure

Thin (1.6 mm thick) and thick (4 mm thick) Al–Li 8090 alloy sheet (composition (wt %) of Al–2.5Li–1.3Cu–0.6Mg–0.12Zr–0.1Fe–0.05Si) were mechanically polished and degreased prior to diffusion bonding (DB) either in the solid state without interlayers, or via a transient liquid phase (TLP) using a thin (~10 µm) copper interlayer (8 µm foil sandwiched between copper sputter-coated sheet surfaces). DB was carried out in a vacuum hot press at 550 °C for 2 h (solid state DB), or 560 °C for 4 h (solid state and TLP DB), under a pressure of 0.75 MPa.

90° “T” peel test pieces were made by bonding a 25 mm length at one end of two test piece blanks 100 mm long by 18 mm wide, and then bending the unbonded arms through 90° at ~500 °C (Figs 1a, 2a). The larger bend radius obtained for thick sheet (Fig. 3a) was associated with a significant bending moment,  $M$ , in Fig. 1b.

Peel tests were carried out (i) in the as-bonded state under SPF conditions at 530 °C at an equivalent strain rate between the pin holes of  $3 \times 10^{-4} \text{ s}^{-1}$  (crosshead speed  $1.7 \text{ mm min}^{-1}$ ; the effect of strain rate was determined by increasing or decreasing the crosshead speed by a factor 10) and (ii) at room temperature and a strain rate of  $3 \times 10^{-4} \text{ s}^{-1}$  in the following conditions; (a) as-bonded, (b) solution heat treated (20 min at 530 °C (SHT), cold-water quench (CWQ)), (c) SHT and aged (5 h at 185 °C, STA), (d) thermally cycled (TC, 1 h, 530 °C), air cooled (AC) and aged.

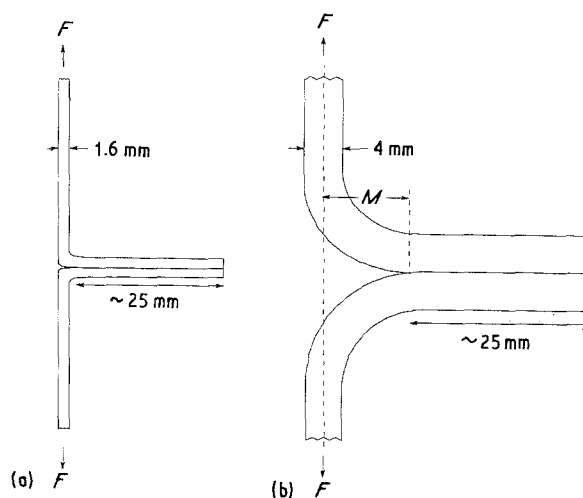


Figure 1 Schematic diagram of diffusion bonded 90° “T” peel test piece: (a) small bend radius, (b) large bend radius showing bending moment,  $M$ .

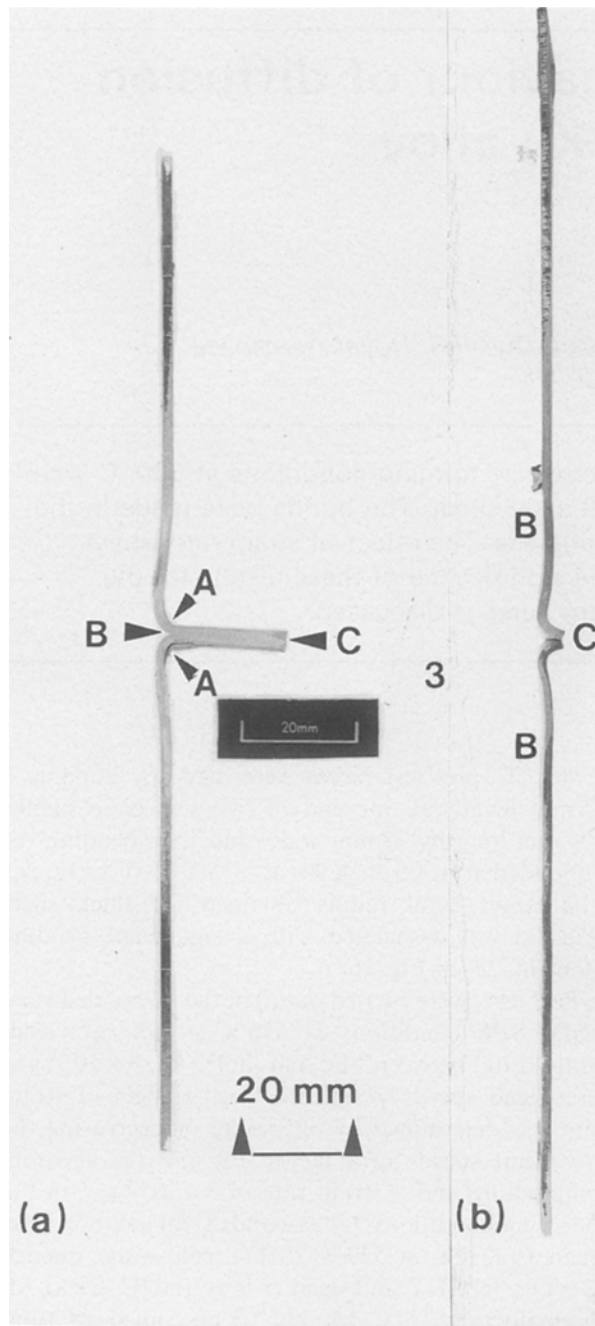


Figure 2 Solid state diffusion-bonded 1.6 mm thick 8090 alloy 90° "T" peel test piece with small bend radius at A; (a) before testing; (b) after almost complete peel fracture (B-C) under superplastic conditions at 530 °C. Crack initiation at B, crack growth direction B-C.

Load versus time curves were converted to peel strength (load/bond width) versus crosshead displacement curves.

### 3. Results

The microstructure of a solid state DB joint in the STA condition (Fig. 4a) showed a planar bond interface (A-A) which was difficult to distinguish from the surrounding grain boundaries. Transmission electron microscopy and selected-area electron diffraction analysis showed this bond interface was a conventional large-angle grain boundary [9]. A non-planar bond interface with a coarser grain microstructure was ob-

tained for a TLP DB joint in the same heat-treated condition (Fig. 4b). Shear strengths of these DB joints at room temperature were similar and about equal to the value for the base metal (190–200 MPa) [2].

#### 3.1. 90° "T" peel tests at 530 °C

Peel strength curves at 530 °C are shown in Fig. 5. Solid state and TLP diffusion-bonded thin sheet test pieces with small bend radii showed peaks in their peel strength curves followed by steady state peel plateaus at lower strengths. The curve peak was absent or much less marked with thicker sheet test pieces. Peel crack nucleation occurred at the load peak or at the onset of steady state peel.

During steady state peel of solid state bonds in 1.6 mm sheet at the plateau stress, the bend radius remained about  $2.5t$  ( $t$  = sheet thickness) irrespective of the initial radius and complete straightening of the test piece arms occurred (Figs 2a, b, 3a, b). The peel crack growth rate under these conditions is equal to half the crosshead speed, i.e.  $\sim 1.7/2 = \sim 0.85 \text{ mm min}^{-1}$ . The absence of a peak and the lower plateau for thicker sheet is attributed to the greater moment arm associated with the greater bend radius in thick sheet (Figs 1b, 3a). The TLP DB joints had lower peel strengths than solid state bonds (Fig. 5 and Table I).

The shape of peel test pieces after testing depended on peel strength and sheet thickness. The bending in the arms of 4 mm thick sheet test pieces was much less for the weaker TLP DB joint as shown by the larger bend radius in the latter (Fig. 3b, c), and this joint failed after a smaller crosshead displacement than for the solid state joint (Fig. 5).

A solid state joint between thick and thin sheet is shown before and after testing in Fig. 6. The peel angle developed in the thinner sheet reached about 135° and the force exerted by the sheet was sufficient to almost straighten the thicker sheet. Note, however, that the peel strength curve for this test piece coincided with the plateau for thin sheet (Fig. 5) and was stronger than the equivalent 4 mm thick joint.

Peel strengths were also dependent on crosshead speed for both solid state and TLP DB joints. The peel strength effectively increases with increase in peel crack growth rate,  $C_r$  (crosshead speed/2) (Fig. 7) according to the relationship

$$P = kC_r^z \quad (1)$$

where  $k$  is a constant (equal to 0.66–0.71 and 0.36 N min for solid state and TLP bonds, respectively) and  $z$  is a crack growth rate exponent (with values in the range 0.27–0.33). Since during transient changes in cross-head speed the test piece geometry is unchanged, the change in peel crack growth rate must be caused by the strain rate dependence of the plastic deformation and fracture at the peel crack tip. This is consistent with  $z$  being independent of sheet thickness and bond type whilst  $k$  reflects the bond strength. The effect of crosshead speed is significant, e.g. an increase in the cross-head speed by a factor 20, or the peel crack growth rate by a factor 10, will double the

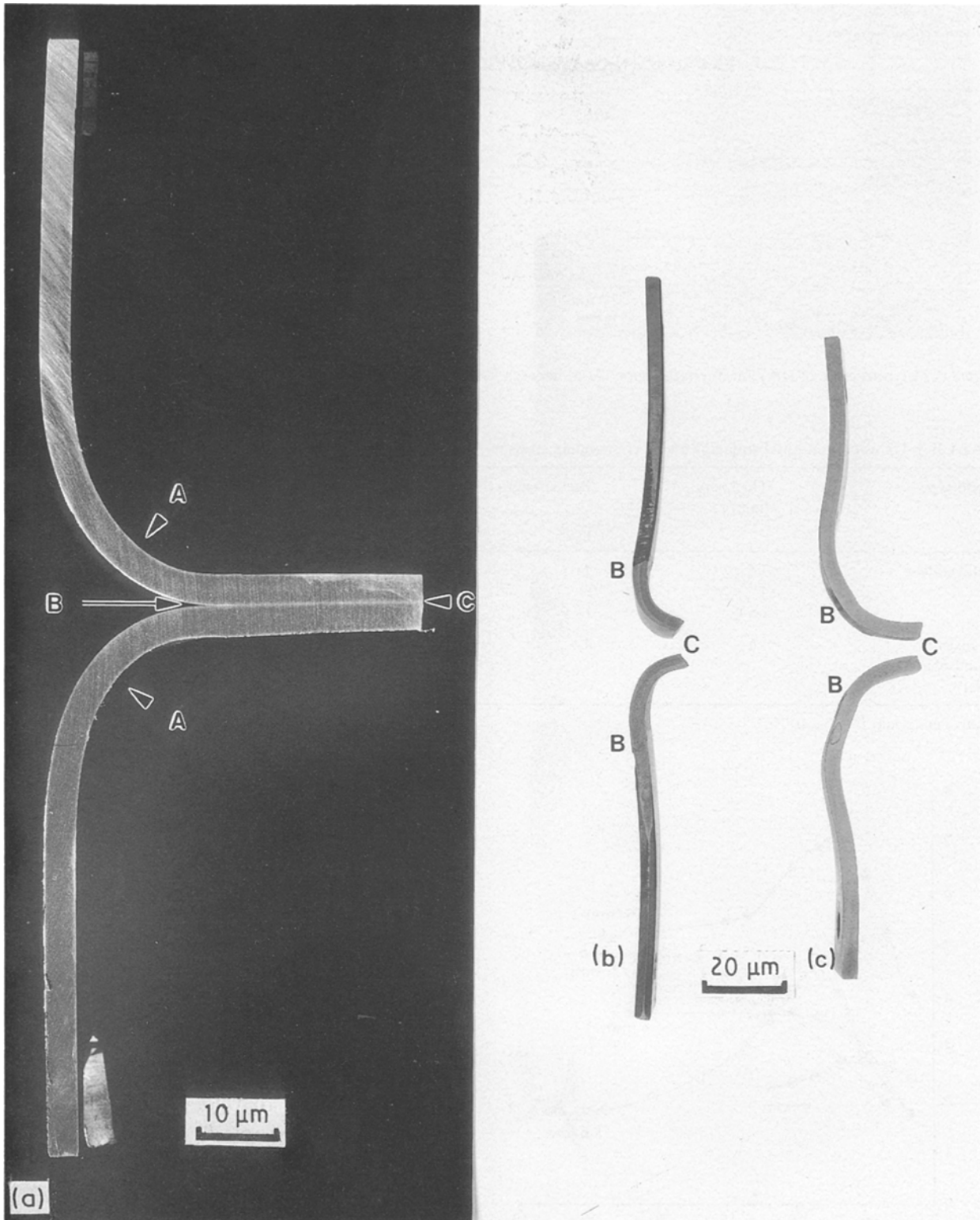


Figure 3 Diffusion-bonded 4 mm thick 8090 alloy 90° "T" peel test piece with large bend radius at A: (a) before testing. Solid state DB (b) and TLPDB (c) after peel fracture under superplastic conditions at 530 °C. Crack initiation at B, peel fracture B-C.

measured peel strength. This has not been recognized previously [4, 5].

### 3.2. 90° "T" peel tests at room temperature

Room-temperature peel strengths were independent of sheet thickness in both solid state and TLP diffusion-bonded joints and independent of bonding temperature for solid state diffusion-bonded joints.

The characteristic peak and plateau peel strength curves were obtained for material in the high-strength

condition, e.g. STA (Fig. 8) or TC + AC + age. For a 1.6 mm thick solid state DB test piece peaks in the range 54–31 N mm<sup>-1</sup> were followed by plateaus in the range 18–15 N mm<sup>-1</sup>. For a TLP bond the peak and plateau values were lower at 16 and 8 N mm<sup>-1</sup>, respectively. No curve peaks were obtained for softer conditions (as bonded or SHT) when plateau peel strengths were 70 N mm<sup>-1</sup> for solid state DB test pieces (Fig. 8). Note these values were much higher than the corresponding values for the harder condi-

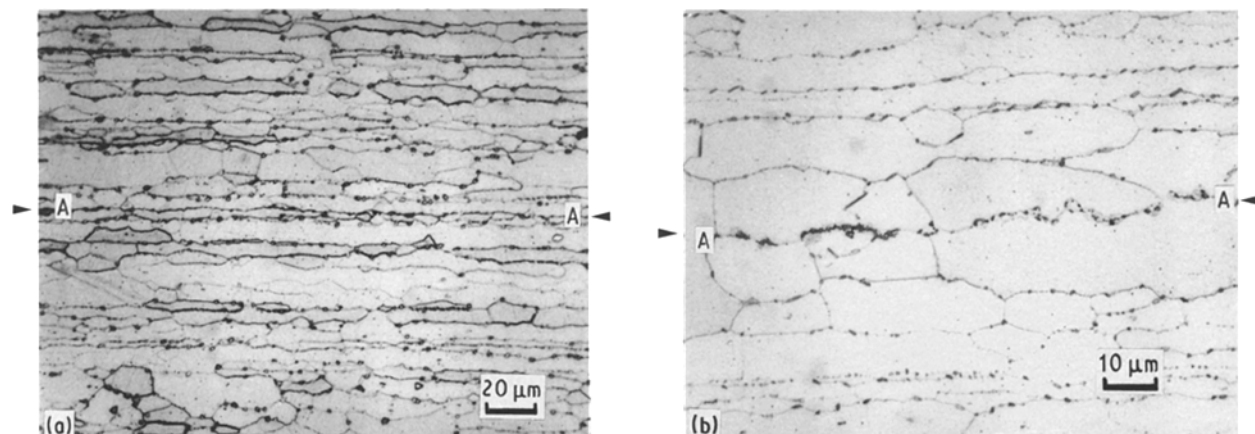


Figure 4 Microstructure of DB joint interface region (A-A) between 8090 alloy: (a) solid state, (b) TLP.

TABLE I Diffusion-bond peel strengths and corresponding stress in the test piece arms at 530 °C

Bond type	Thickness (mm)	Peel strength ( $\text{N mm}^{-1}$ )		Corresponding stress in test piece arms (MPa)
		Peak	Plateau	
Solid state	1.6	7	5.2	4.4, 3.3
	4		3.5	0.85
	1.6/4		4.8	3/1.2
Transient liquid phase (TLP)	1.6	4.4	1.9	2.75, 1.2
	4		2.2	0.55

Equivalent strain rate  $3 \times 10^{-4} \text{ s}^{-1}$ .

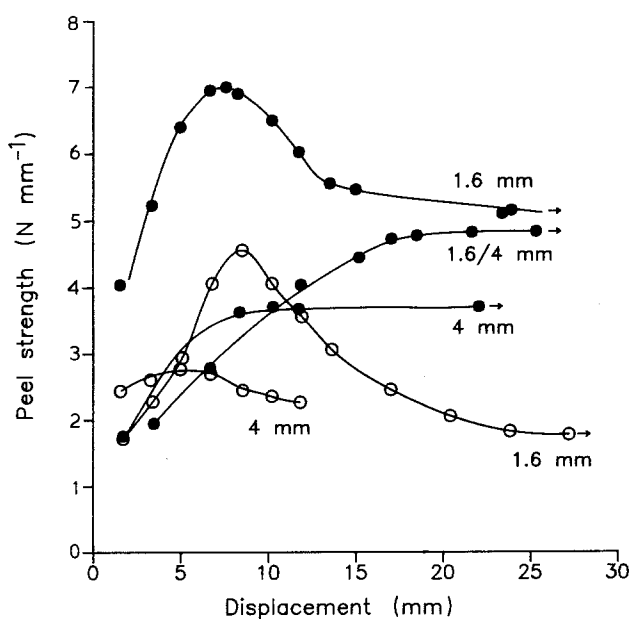


Figure 5 Peel strength versus displacement (crosshead) curves showing the effect of test piece thickness for (●) solid state and (○) TLP DB joints at 530 °C.

tions. The SHT TLP bond had a lower plateau value at  $40 \text{ N mm}^{-1}$ . The peel strength data are summarized in Table II.

Plastic bending of the test piece during testing at room temperature was much less than at 530 °C as shown in Fig. 9, and decreased as the strength of the sheet increased. During peel fracture in the STA con-

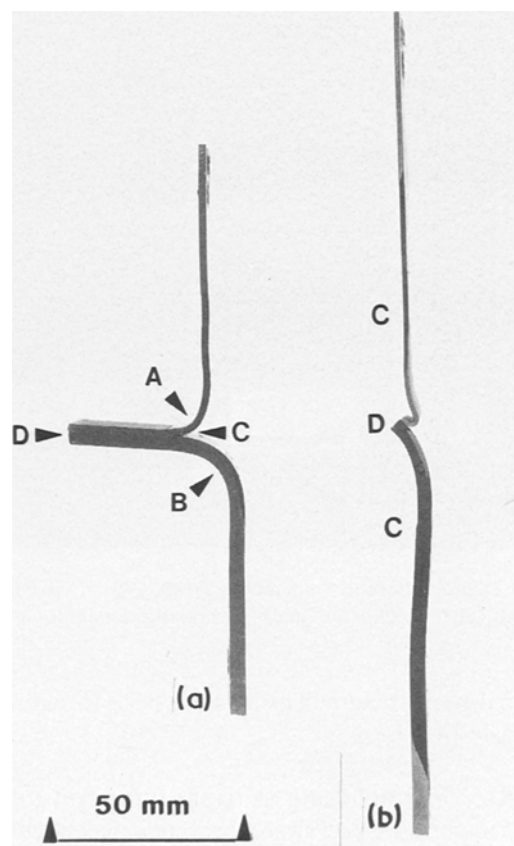


Figure 6 Solid state diffusion-bonded 1.6–4 mm thick sheet test piece with small bend radius at A and large bend radius at B: (a) before testing; (b) after almost complete peel fracture (C–D) under superplastic conditions at 530 °C. Crack initiation at C.

TABLE II Diffusion-bond peel strengths at room temperature

Bond type	Thickness (mm)	Heat treatment condition	Peel strength ( $\text{N mm}^{-1}$ )	
			Peak	Plateau
Solid state	1.6, 4	As-bonded		70
	1.6, 4	SHT		70
	1.6, 4	(Solution heat treated)	31-48	15
	1.6	STA	54	18
Transient liquid phase (TLP)	4	SHT		40
	4	STA	16	8

Equivalent strain rate  $3 \times 10^{-4} \text{ s}^{-1}$ .

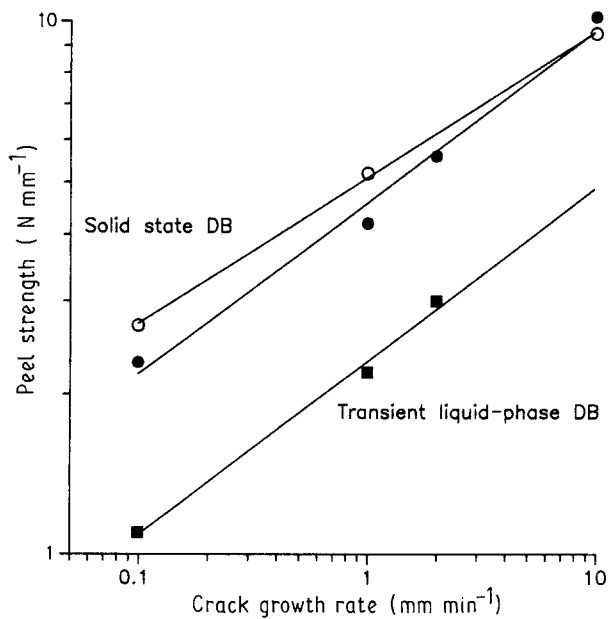


Figure 7 Peel strength versus crack growth rate (strain rate) for solid state and TLP diffusion bonds tested under superplastic conditions at 530°C. Sheet thickness: (○) 1.6 mm, (●, ■) 4 mm.

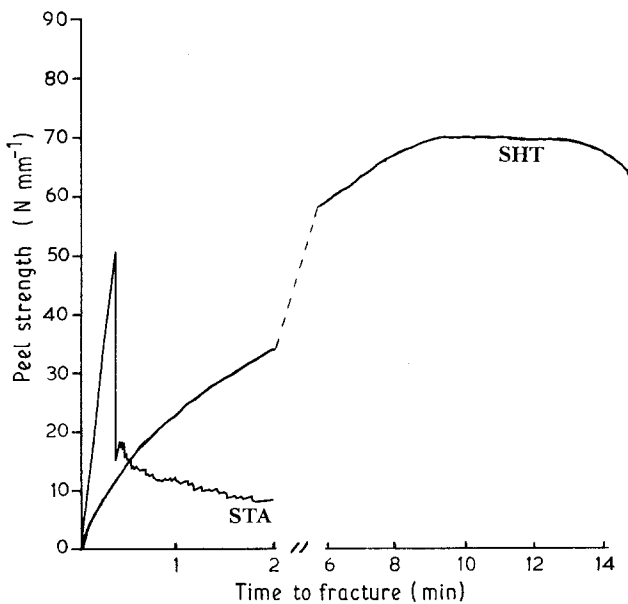


Figure 8 Peel strength versus time to fracture for solid state bonds at room temperature in the SHT and STA conditions.

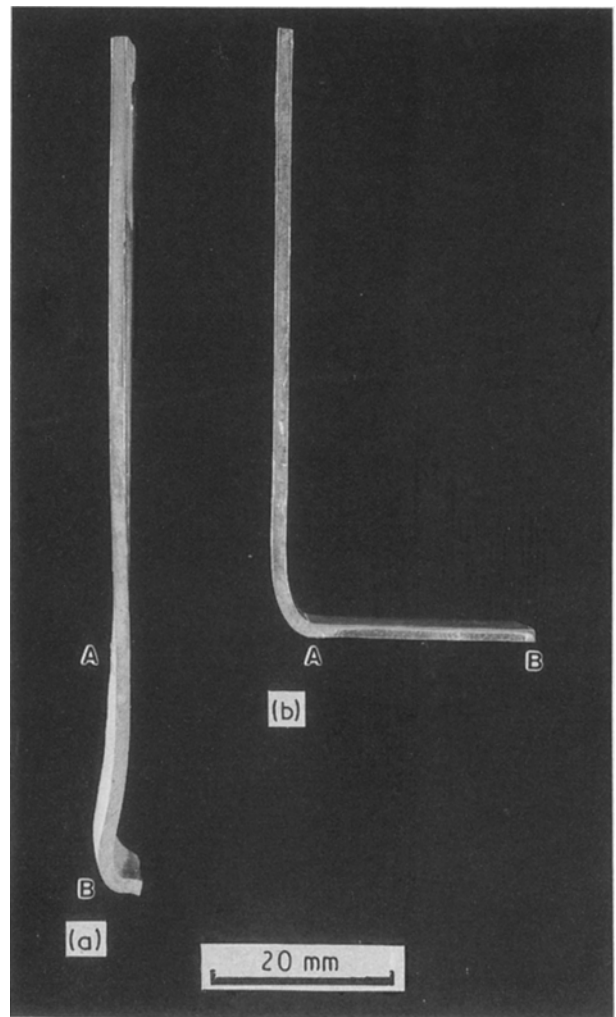


Figure 9 Plastic bending associated with peel fracture for 1.6 mm sheet. Peel fracture A-B. (a) Tested under superplastic conditions at 530°C; (b) tested in the STA condition at room temperature.

dition at room temperature no significant change in the shape of the test piece was apparent (Fig. 9).

Peel crack growth rates were measured during peel fracture in the plateau stage by monitoring the crack tip displacement at the edge of the bond plane. Crack growth rates depended on the amount of plastic bending of the sheet. Values of about 20 and  $1.5\text{--}2 \text{ mm min}^{-1}$  were obtained for sheet in the STA and SHT conditions, respectively. The rate for the

SHT test piece is about twice that for steady state crack growth at 530 °C. When the bond plane remains almost flat in the STA test piece, with little macroscopic plastic bending of the sheet at the crack tip, small crosshead displacements lead to much faster peel crack growth rates. This difference in crack growth rate is reflected in the much shorter time to fracture for material in the STA condition (Fig. 8).

### 3.3. Peel fracture

Surface studies were carried out on the test piece fractured in the STA condition. (Oxidation on exposed surfaces at elevated temperatures obscured fractures made at 530 °C). Extensive plastic deformation of the sheet surface at the edge of the bond plane and adjacent to the fracture surfaces was observed (Fig. 10) and wavy parallel peel fracture striations (A–A in Fig. 11a) were oriented perpendicular to the crack direction; the latter are consistent with crack growth in increments of 0.1–0.2 mm. At high magnification the fracture surface showed almost deformation-free intergranular fracture at the bond interface grain boundary (B in Fig. 11b, c), which is a characteristic fracture mode for bonds in this alloy sheet [8]. In some regions the crack had deviated from the bond plane to a depth of about 2–4 grains to produce pits and hillocks at C and D, respectively, in Fig. 11. The fracture in the base of the pit (at E in Fig. 11) was much rougher because of the less planar grain boundaries in the base metal [8]. The tendency for the crack to wander out of the bond plane indicates the bond interface peel strength was about the same as that for the base metal, in agreement with bond shear fracture data for this alloy [8].

## 4. Discussion

In the stress analysis of peel test pieces elastic behaviour is normally assumed and for flexible joints an energy balance approach is often preferred [10, 11]. The work done,  $W$ , by the peel force during steady state peel is used to create two fracture surfaces and

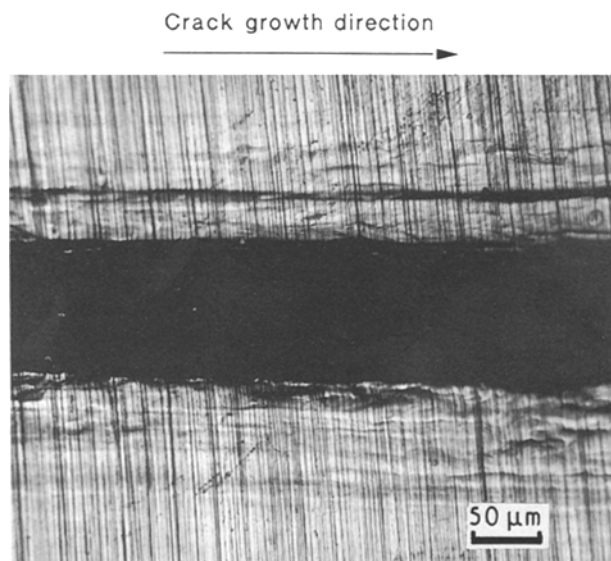


Figure 10 Surface deformation on the edge of a solid state DB test piece after peel fracture in the STA condition at room temperature.

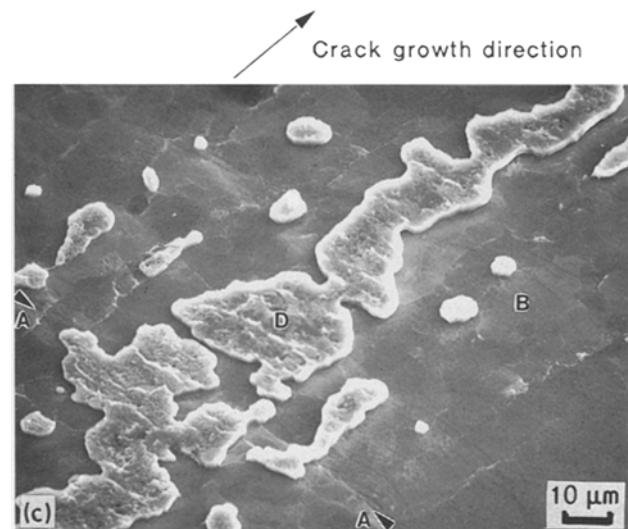
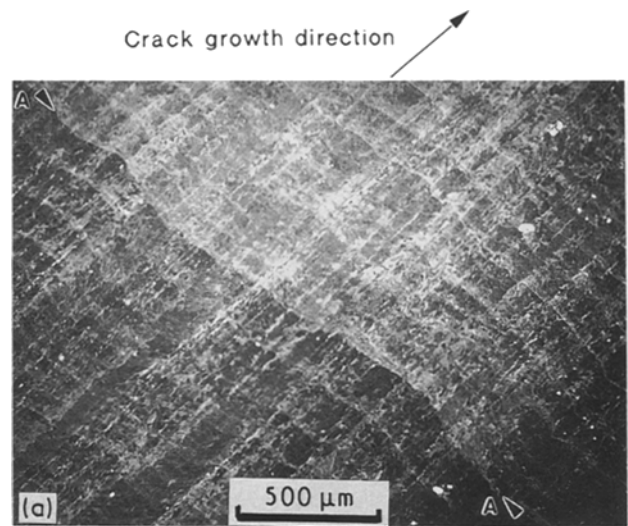


Figure 11 Scanning electron micrograph of a solid state diffusion bond after peel fracture in the STA condition at room temperature. (a) Fracture striations, (b) pit, (c) hillocks.

the interfacial fracture energy per unit area,  $W_d$ , is given by

$$\begin{aligned} W_d &= Fdl/wdl \\ &= F/w \\ &= PN \text{ mm}^{-1} \end{aligned} \quad (2)$$

where  $F$  is the peel force,  $w$  the width of the crack,  $dl$  the advance of crack and  $P$  the peel strength. In practice, the peel of DB joints is more complex and the peel force is not a direct measure of the fracture energy. Plastic bending,  $W_b$ , crack tip plasticity,  $W_{ct}$ , and superplastic deformation,  $W_{spf}$ , at elevated temperatures can lead to a significant increase in the energy dissipation during a peel test with a consequent increase in the peel strength, i.e.

$$P = W_{spf} + W_b + W_{ct} + W_d \quad (3)$$

In a 90° peel test with adhesively bonded thin metal films, 98% of the energy for steady state peel was used to plastically deform the adherend [12]. The present tests have shown that for a given diffusion-bond strength the measured peel strength curves at 530 °C may or may not exhibit peaks, and can have different strength levels for the peaks and plateaus depending upon the ease of plastic deformation, which in turn depended upon the sheet thickness, bend radius and crosshead speed (Fig. 5). It is therefore important to take account of the first three terms in Equation 3 when using the peel test to compare the effect of processing variables on the actual bond strength.

The strength of solid state diffusion-bonded joints was greater than that of TLP diffusion-bonded joints made with ~ 10 µm copper interlayers and tested under identical conditions (Tables I and II). Other reported peel test data for a TLP joint formed with a zinc interlayer [4] are compared in Fig. 12. At 530 °C, the TLP joints exhibited similar peak/plateau curves; the slightly higher plateau for the zinc interlayer could be caused by the higher strain rate used. The reported TLP strength [4] was based upon the peak strength which was about twice the plateau strength. However, peel crack nucleation has been shown to occur at the peak strength with thin sheet test pieces and at the plateau strength with thicker sheet. It may therefore be unwise to quote a hot peel strength for 8090 alloy based

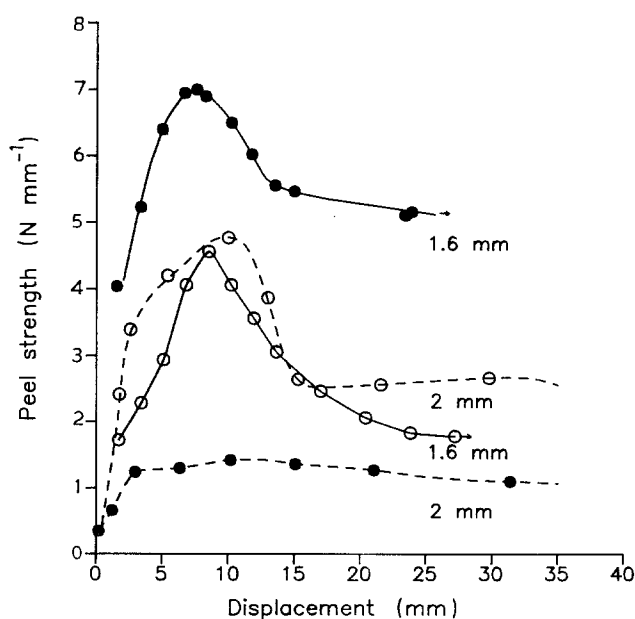


Figure 12 Peel strength versus displacement (crosshead) curves for thin sheet. (—) At 530 °C, present work, (---) [4], (●) solid state DB, (○) TLP DB.

on a load peak. Note the much lower peel strength reported for the solid state bond. This is consistent with the reported shear strength at room temperature [4], which was a factor 4 lower than that obtained in the present tests. These comparisons emphasize the variability in published data and the need for agreement on the testing and analysis of diffusion-bonded joints. For comparison, peel strengths measured at room temperature for adhesive bonded aluminium alloy joints are about 8 N mm<sup>-1</sup> [13].

The 530 °C test data in Table I indicate that 90° peel fracture will occur before the superplastic flow stress of 5 MPa is reached in 1.6 mm sheet. Thus, for DB/SPF the bond strength is critical for 90° bonded joints in sheet thicker than about 1 mm. However, other work has shown [14] that for the high bond strengths obtained in the present tests the bonded joint strength may cease to be critical with angles of less than 90° and different joint designs.

## 5. Conclusions

90° peel strengths at room temperature and at 530 °C for solid state and TLP diffusion-bonded joints were significantly higher than those reported for adhesive-bonded joints. Solid state-bonded joints were stronger than TLP joints. Peel strengths were sensitive to the amount of plastic deformation, and this depended on sheet thickness, heat treatment and strain rate. It was concluded that for sheet thicker than about 1 mm, peel fracture of 90° joints would occur before deformation of the sheet at ambient temperatures and at 530 °C.

## Acknowledgements

The authors thank Dr McDarmaid for many useful discussions. This paper is published with the permission of the Controller, Her Majesty's Stationary Office, London, 1991, holder of Crown Copyright.

## References

1. R. GRIMES, B. J. DUNWOODY and J. A. JONES, in "Superplasticity in Metals, Ceramics and Intermetallics", Vol. 196, edited by M. J. Mayo, M. Kobayashi and J. Wadsworth (Materials Research Society, PA, 1990) pp. 167-72.
2. D. V. DUNFORD and P. G. PARTRIDGE, *J. Mater. Sci.* **25** (1990) 4957.
3. D. W. LIVESEY and N. RIDLEY, "Diffusion Bonding 2", edited by D. J. Stephenson (Elsevier, 1991) pp. 83-100.
4. R. A. RICKS, G. J. MAHON, N. C. PARSONS, T. HEINRICH and P.-J. WINKLER, *ibid.*, pp. 69-82.
5. H. M. TENSI and M. WITTMAN, *ibid.*, pp. 101-10.
6. D. STEPHEN, "Designing with Titanium" (Institute of Metals, London, 1986) pp. 108-24.
7. K.-S. KIM and J. KIM, *Trans. ASME* **110** (1988) 226.
8. D. V. DUNFORD and P. G. PARTRIDGE, *J. Mater. Sci.* **26** (1991) 2625.
9. C. J. GILMORE, D. V. DUNFORD and P. G. PARTRIDGE, *ibid.* **26** (1991) 3119.
10. A. J. KINLOCH, "Adhesion and Adhesives: Science and Technology" (Chapman and Hall, London, 1987) p. 191.

11. J. J. BIKERMAN, "The Science of Adhesive Joints" (Academic Press, New York, 1968) pp. 242-63.
12. K.-S. KIM, "Adhesion in Solids", Vol. 119, edited by D. M. Mattox, J. E. E. Baglin, R. J. Gottschall and C. D. Batich (Materials Research Society, PA, 1988) pp. 31-41.
13. A. J. KINLOCH, *J. Mater. Sci.* 17 (1982) 617.
14. D. V. DUNFORD and P. G. PARTRIDGE, *J. Mater. Sci.* (1992) in press.

*Received 24 July  
and accepted 30 July 1991*